Identification of Styryl Sulfonyl Fluoride (SSF) as An Efficient, Robust and Irreversible Cysteine-specific Protein Bioconjugation Reagent

Qingsong Wu[1], Qi Xue[1], Ji Li[1], Qinheng Zheng[2], Xinlu Zhao[1], Wannan Li[1], Shiming Sun[1], Wanxing Sha[1], Yang Yang[1], Yi Yang[3], Jie P. Li[1]*

[1]State Key Laboratory of Coordination Chemistry, Chemistry and Biomedicine Innovation Center (ChemBIC), School of Chemistry and Chemical Engineering Nanjing University 163 Xianlin Avenue, Nanjing, Jiangsu 210023, China, E-mail: jieli@nju.edu.cn
[2]Cellular and Molecular Pharmacology, University of California San Francisco, 600 16th Street，San Francisco, CA 94143 USA
[3]Glyco therapy Biotechnology Co., Ltd, 12 606 Bio village, 291 Fucheng Road, Xiasha street, Qiantang Distirct, Hangzhou, Zhejiang, 310058, China

ABSTRACT: Cysteine (Cys)-specific bioconjugation has found wide application in the synthesis of protein conjugates, particularly for the functionalization of antibody. Here, through direct assessment on protein substrate, we report the discovery of *trans*-styryl sulfonyl fluoride (SSF) as a near perfect Michael acceptor (MA) for cysteine-specific protein bioconjugation. Compared to predominantly used maleimides, SSF exhibited better chemoselectivity, self-stability and conjugate-stability while kept comparable reactivity. Using SSF-derived probes, proteins can be readily modified on the Cys residue(s) to install functionalities, *e.g.*, fluorescent dyes, toxins and oligonucleotides (oligos), without the influence of activity. Further applications of SSF derived serum stable antibody-drug conjugates and PD-L1 nanobody-oligo conjugates demonstrate the great translational value of SSF-based bioconjugation in the drug development and single-cell sequencing.

INTRODUCTION

The development of bioconjugation techniques has become a cornerstone for the advancement of chemical proteomics[1], biomaterial synthesis[2], biomolecular imaging[3], single-molecule analysis[4], single-cell multi-omics[5] and multispecific drugs[6]. Despite the emergence of bioconjugation reactions that utilize different natural and unnatural amino acids in protein molecules[7], cysteine (Cys)-specific conjugation remains the most widely used strategy for native protein modification[8]. This is due to the unique nucleophilicity and the low natural abundance of Cys residues, which provides opportunities for rapid and selective protein modifications[9]. Various types of reactions have been reported to specifically label Cys in proteins, including alkylation[10], arylation[11] and Michael additions[12]. Among these, Michael addition appears a more favorable chemistry in application due to its fast reaction kinetics in aqueous buffer. Notably, seven of twelve FDA-approved antibody-drug conjugates (ADC) are constructed via the Michael addition reactions between Cys and maleimide[13].

Although maleimide has been widely used in protein labeling since the discovery in the 1950s[14], the thiol-maleimide reaction is limited by several drawbacks. First, maleimide may react with amine at higher pH to generate heterogenous mixtures of conjugates, which links to the residue of Cys or Lysine (Lys)[12]. Second, the hydrolysis of maleimide in alkaline solution results in an unreactive maleamic acid, which requires strict storage conditions for maleimide reagents[15]. Most importantly, thiol-maleimide adducts are not resistant to biochemical nucleophiles, and easily decompose in clinically relevant samples[16]. Continuous efforts have been made to find a perfect Michael acceptor (MA) for Cys-specific protein modifications, which could balance the properties of reactivity, self-stability, chemoselectivity as well as the stability of adducts[17].

In the development of protein chemistry, organic reactions under mild conditions inspire chemists to discover novel bioconjugation strategies[18]. To discover potentially better MAs in protein bioconjugations, we pay attention to the Mayr's database that summarizes a series of MAs of substituted ethylenes for prediction of reactions in organic synthesis, which is little used in protein chemistry[19]. We envision that MAs from this database could be comprehensively interrogated on proteins to novel Cys-specific bioconjugation reagents. Through the direct assessment of protein reactions in a LC-MS-based platform, we herein report on trans-styryl sulfonyl fluoride (SSF) as a near perfect MA for Cys-specific protein conjugation. SSF derived functionalities were used to generate serum stable protein conjugates efficiently, and shows better reactivity than current platforms for stable ADC construction in clinical stage. Moreover, SSF modified functionalities, e.g., SSF- single-stranded DNA (ssDNA), are quite stable in aqueous buffer, which provides a novel readily reactive reagent for the construction of DNA-protein conjugates (**Fig. 1**). Further performance characterization shows the promising translational value of this chemistry in preparing protein conjugates for applications of single-cell omics and novel ADC therapies.

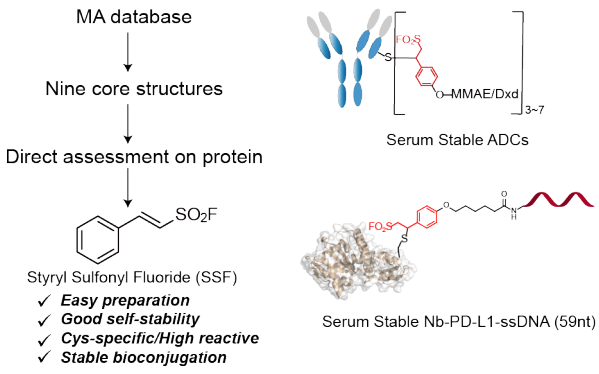

Figure 1. Scheme for FDA-approved ADCs using cysteine-specific conjugation.

RESULTS AND DISCUSSION

Identification of SSF from the database of acceptor-substituted ethylenes.

We initiated our studies by selecting acceptor-substituted ethylenes from the database of electrophiles. Nine compounds (**MA1-9**) representing core structures of 114 substituted ethylenes are selected for characterization in reaction with protein (E value represents the electrophilicity[20]) (**Fig. 2A**). Some structures are virtually excluded due to their steric hindrance and instability. Green fluorescent protein (GFP) with a highly reactive Cys mutation (E124C, referred as GFP hereafter) was directly used as the protein substrate in comparing these MAs, in which total of three Cys residues could be modified ($N_{Cys=3}$) (**Fig. 2A**). We first characterized the reactions between GFP and **MA1-9** (50 equiv.) in PBS buffer (pH 7.4) by LC–MS analysis. Surprisingly, **MA5-9**, though less electrophilic (low E value) than **MA1-4**, showed higher reactivity towards GFP, in which average modification numbers (mod#) are more than one (**Fig. 2B, Fig.S1**). By contrast, **MA1-4** bearing high *E* values displayed low reactivity (mod# <1) or complex reaction profiles. Similar results could also be observed at higher pH (pH 9.0), although **MA1** and **MA4** showed a slightly improved reaction efficiency (**Fig. 2B**, **Fig.S1**). Furthermore,. when reduced IgG antibody were used as protein substrates, **MA1-9** showed complex reaction profiles again and only **MA5-7** showed consistent reactivity on GFP and IgG (**Fig. S2**). We speculate that local chemical environments of Cys on the protein may affect the reactivity of **MA1-4**. To examine this hypothesis, we next performed Michael additions with **MA1-9** on peptides without complex strutures in 50% (v/v) CH_3CN/PBS (**Table S1-S2**). As expected, most of MAs reacted with cys-bearing peptides, and their reactivity generally followed the trend of their electrophilicity, which supports our hypothesis that the local environment of Cys residues affect their reactivity with MAs. Among the reactive MAs identified on GFP modification, **MA7** reacted with more than three residues on GFP (mod#>N_{Cys}), and there are additional non-Cys- specific modifications at pH 9.0 (**Fig. 2B**, **Fig.S1**), reflecting its poor chemoselectivity. As indicated in previous work, maleimide (**MA5**) displayed a slight non-Cys-specific modifications (mod#> NCys) at pH 9.0 as well (**Fig. 2B**)[12]. Thus, we chose **MA6, MA8** and **MA9** to further evaluate the

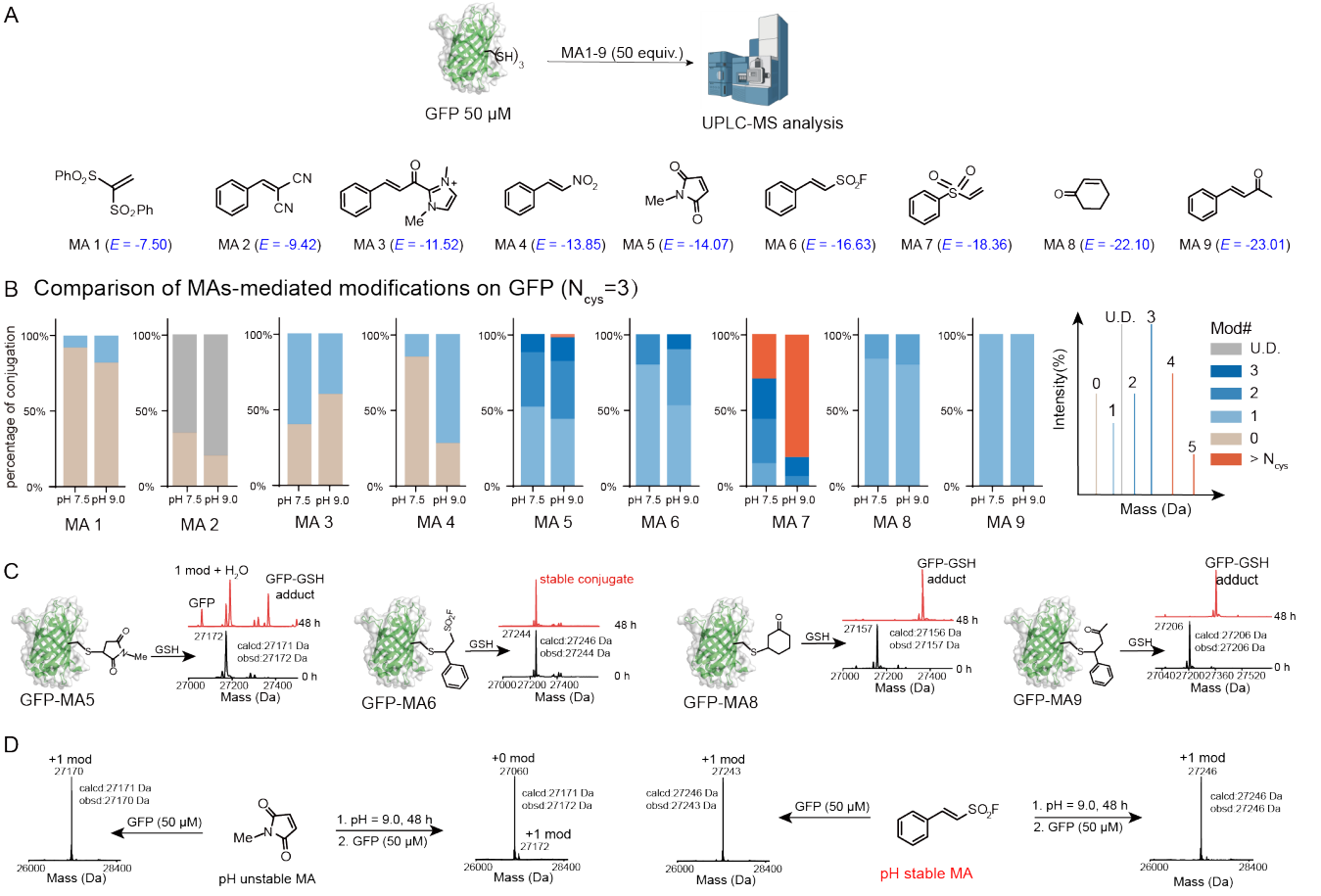

Figure 2. Comparison of representative MA-mediated modifications on proteins. A) Reaction scheme for **MA1-9** with GFP. B) Reaction profiles of GFP with MAs. Shown are percentages of GFP conjugate with indicated modification numbers. Reaction conditions: 50 μM GFP, 2.5 mM **MA1-9**, PBS buffer (50 mM, pH = 7.4/9.0), 37°C, 2 h. **MA2** conjugate cannot be assigned, which is probably due to the potential elimination of the CN group after reaction. Electrophilicity *E* from Ref20. C) Stability of GFP-MA conjugates when exposed to GSH treatment. Reaction conditions: 2 mM GSH, 20 μM GFP-MAs, PBS, 37°C for 48 h. D) Hydrolytic stability of **MA 6** versus **MA5.**

stability of their conjugates in the presence of 2 mM GSH (**Fig. 2C**). Maleimide was included as a control in all of following comparisons due to its wide applications. Impressively, only the GFP-MA6 (SSF) conjugate exhibited complete stability in 48 hours. SSF was then compared with maleimide in alkaline buffer to characterize the self-stability. As expected, the hydrolysis of maleimide at pH 9.0 resulted in the unreactive product, but SSF kept the reactivity even treated at pH 9.0 for 48 h and reacted with GFP at C124 completely (**Fig. 2D**). Together, by comparing the reactivity, selectivity and conjugate-stability, SSF stands out from nine core structures of substituted ethylenes.

Comparison of SSF analogues in protein bioconjugations.

In recent years, Sharpless and co-workers recognized that ethenesulfonyl fluoride (ESF) "ranks at the top of the reactivity hierarchy of known Michael acceptors", and developed methodologies for the synthesis of ESF analogues[21]. Meanwhile, the Mayr group confirmed that ESF is among the strongest MAs on their comprehensive electrophilicity scale using physical organic approaches.[22] As **MA6** (SSF), a derivative of ESF, shows a great balance of reactivity, selectivity and stability towards modifying Cys on protein, we sought to systematically study ESF analogues to expand our knowledge of these MAs in protein reactions (**Fig. 3A**). We prepared four alkenyl sulfonyl fluorides (**MA10-13**) bearing substituted ethene structures as analogues of SSF and they all showed good reactivities toward GFP except 1,2-disubstituted vinyl sulfonyl fluorides (**MA13**) (**Fig. 3B**). Although (*Z*)-2-phenylethenesulfonyl fluoride (**MA10**) and 1-phenyl ethenesulfonyl fluoride (**MA11**) were very reactive, their poor residue selectivity (mod# > N_{cys}) prevented their further application. We also included analogues that replace the fluoride linked to sulfonyl with CF_3 and CH_3 (**MA14** and **15**). Unexpectedly, both of these MAs show lower reactivity towards GFP regardless of whether the substitution is electron-donating or electron-withdrawing (**Fig. 3B**). It seems that the unique property of fluoride substitution leads to the high electrophilic reactivity of ESF analogues, which might be a combination of electronic and steric effects. Moreover, the subsequent competition assay identified **MA6** as a more reactive Michael acceptor than β-alkyl vinyl sulfonyl fluoride (**MA12**) (**Fig. 3C**). These results indicate that **MA6** has the most balanced reactivity and selectivity among all the ESF analogues that we tested. Further alkyl azide substituent (**MA16**) on the phenyl group of **MA6** shows equal reactivity as its parent compound, which facilitates the further functionalization of SSF via click chemistry (**Fig. 3C**).

Characterization of SSF reactivity and specificity on diversified proteins

There are a couple of reported Cys-specific labeling reagents in the clinical stage for constructing serum stable protein conjugates[17e, 17h]. To compare their reactivity with SSF, we monitored their reaction with GFP at different time points (**Fig. S3**). Remarkably, the reaction was completed in less than 5 min using 5 equiv. of **MA6** at 37°C, much more effective than others, which is consistent in modifying other proteins (**Fig. S4**). For example, neo2 (a *de novo* cytokine mimic of IL2,14 KDa)[23], Nb-PD-L1 (PD-L1 nanobody, 15 KDa)[24], trastuzumab (HER2 targeted monoclonal antibody, 150 KDa)[25], KN026 (biparatopic HER2 targeted antibody, 150 KDa)[26] and KN046 (bispecific antibody that blocks PD-L1 and CTLA-4, 110 KDa)[27] were all modified in full conversion (**Fig. 4A-B, Fig. S5**), but

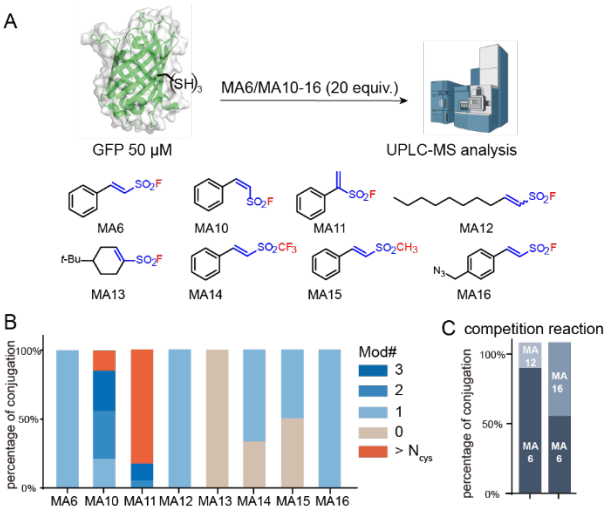

Figure 3. Comparison of **MA6** with its analogues. A) Reaction scheme for **MA6**, **MA10-16** with GFP and chemical structures of **MA6** analogues. B) Reaction profiles of GFP with MAs. Shown are percentage of indicated modification numbers. Reaction conditions: 50 μM GFP, 1 mM **MA6**, **10-16**, PBS buffer, 37°C, 2 h. C) Competition reaction of **MA6** with **MA12**, **MA16**, respectively. Shown are percentages of indicated conjugation. Conditions: 500 μM **MA6**, 500 μM **MA12** or **MA16**, 50 μM GFP.

other reagents only labeled part of Cys residues (**Fig. S4**). The modification numbers of these proteins were characterized, which were found the same as the number of Cys residues they contain, indicating the Cys selectivity during modification. Cys specificity was further confirmed by tryptic digestion followed by LC–MS/MS analysis of protein conjugates (**Fig. 4C**). To demonstrate that the modification did not change the activity of proteins, we characterized recognition ability of SSF-modified trastuzumab, which binds to the HER2 antigen with similar affinity of unmodified trastuzumab (**Fig. 4D**).

Synthesis and application of functionalized SSF reagents

For the further application of this chemistry, an SSF-biotin probe (**MA16-biotin**) was synthesized for the modification of trastuzumab with functionalities (**Fig. S6**). The success of biotinylation on trastuzumab was confirmed by western blot and LC–MS analysis (**Fig. S6 B-C**). We also used this conjugate to facilitate the discrimination of HER2-positive or HER2-negative cancer cells via flow cytometry analysis (**Fig. S6D**). Moreover, a two-step method was applied to modify trastuzumab with the fluorescent dye Cy5.5 through **MA16**-enabled Michael addition followed by strain-promoted azide-alkyne cycloaddition with DBCO-Cy5.5. Labeled proteins were then detected and quantified via in-gel fluorescence scanning of SDS–PAGE gels and LC–MS analysis (**Fig. S6E-F**). Trastuzumab-MA16-Cy5.5 was also used to stain cocultured NCI-N87 and MDA-MB-231 (GFP+) cancer cells. Fluorescence imaging confirmed that strong fluorescence from Cy5.5 appeared only on NCI-N87 cells since they expressed high levels of HER2 antigen (**Fig. S6G**). Together, these results demonstrate the utility of our new bioconjugation method for the generation of functional antibody conjugates.

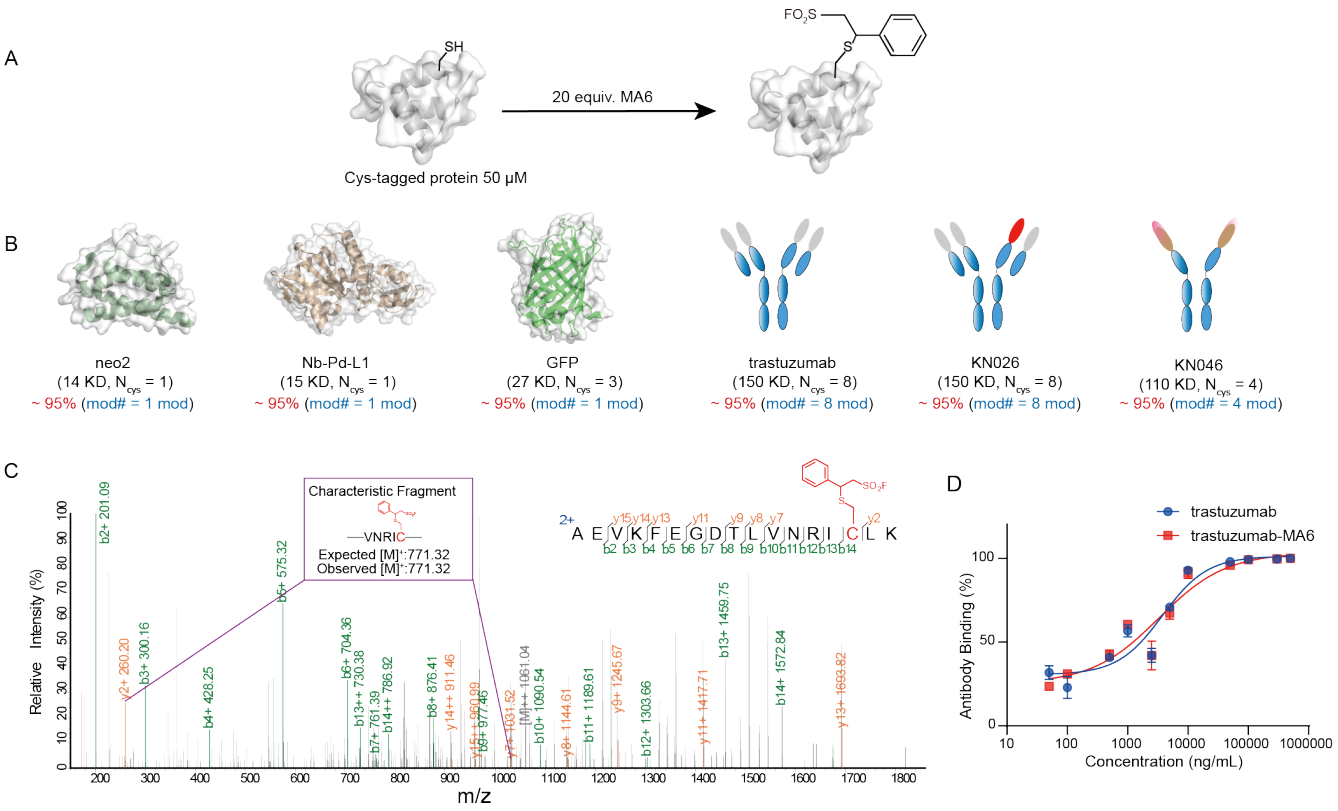

Figure 4. Cys-specific modification of different proteins via SSF. A) Reaction scheme. B) Cys-specific protein modifications with MA6 on the following proteins: neo2, Nb-PD-L1, GFP, trastuzumab, KN026, and KN046. The results were characterized by UPLC–MS. See full spectra in SI. C) MS/MS spectra of GFP fragment modified with MA6. D) Binding affinity of trastuzumab and trastuzumab-MA6 on the HER2+ cell line SKBR3.

Construction of serum-stable ADCs via SSF-Cys conjugation

Having established the foundation for stable Cys-specific protein bioconjugation, we proceeded to use SSF as a reaction handle to construct stable ADCs. We first installed SSF onto a drug linker (vc-PAB-MMAE) to generate SSF-vc-PAB-MMAE (**1**) and then used it to react with trastuzumab (**Fig. 5A-B**). Reaction conditions were screened to generate trastuzumab-**1** with a drug-antibody ratio DAR of approximately 4. As analyzed by LC–MS, 5 equiv. of **1** per antibody were required to reach a DAR of 3.2 at a 5 mg/mL antibody concentration (**Fig. S7-8**). Another ADC synthesized by maleimide-Cys addition was also prepared for comparative purposes since it widely appears in commercial ADCs. Using 3.5 equiv. of Mal-vc-PAB-MMAE (**2**) per antibody, we synthesized trastuzumab-**2** in a DAR of 3.2 (**Fig. S9**). This comparable reaction condition confirmed the high reactivity of SSF. Since the conjugate of SSF-Cys is stable in GSH treatment, we believe that trastuzumab-**1** could show higher stability than trastuzumab-**2**. To prove that under clinically relevant conditions, we next evaluated their stability in human serum *in vitro*. ADCs were incubated with human serum at 37°C for 7 days. After incubation, 90% of trastuzumab-**1** was still stable, while more than 70% of trastuzumab-**2** lost their payload (**Fig. 5C-D, Fig S8-9**). These serum stability data confirm the exquisite stability of trastuzumab-**1**.

Encouraged by this result, we decided to assess the efficacy and safety of trastuzumab-**1**. We started with a cell-based viability assay with the cancer cell lines SKBR3 (HER2+, human breast cancer), and MDA-MB-231 (HER2-, human breast cancer) (**Fig. 5E**). The half maximal inhibitory concentrations (IC50) on SKBR3 cells were similar (10 ng/ml) when using these two ADCs. However, trastuzumab-**2** also inhibited HER2-negative MDA-MB-231 growth at high concentrations (5 μg/ml), while the inhibition was not obvious in the trastuzumab-**1** group. These results indicate that the unstable maleimide-Cys linker of trastuzumab-**2** may lead to unwanted side effects via the release of toxin before binding to cancer cells. To confirm the different bystander killing effects of two these ADCs, we designed a co-culture assay in which SKBR3/MDA-MB-231 mixtures were treated with HER2 targeted ADC to characterize the killing of MDA-MB-231 cells. MDA-MB-231 cells were treated alone as the comparison. Notably, trastuzumab-**2** inhibited the growth of MDA-MB-231 cells in both groups, while trastuzumab-**1** only inhibited the growth of MDA-MB-231 cells in the cocultured group (**Fig. 5F**). These results support that trastuzumab-**1** was more stable in this system and can only induce the bystander killing via the assistance of HER2 positive cancer cells.

To further demonstrate the advantages of the stable SSF-Cys linker *in vivo*, we tested the antitumor efficacy of ADC in NCI-N87 xenograft mouse models (**Fig. 5G, Fig. S10**). To show better activity of stable SSF-ADC, we designed the experiments using a double dose of 1 mg/kg ADC (low dose) at days 0 and 14. To our delight, trastuzumab-**1** showed a slightly better efficacy than trastuzumab-**2** in this condition

according to results from tumor growth inhibition and survival rate experiments (**Fig. 5G-H, Fig. S11**). It is noteworthy that humanized antibodies and vc-PAB linker are not stable in mouse serum (**Fig.5I**, **Fig. S12**), which cause the leveling effect that stable/unstable Cys-linkers could not be discriminated as significantly as expected in human samples. To gain further insights into safety issues of ADC arising from the stability of the linker, we conducted an exploratory study in rats (**Fig. 5J**). Before and after ADC dosing (20 mg/kg), blood samples were taken for hematology analysis. Neutropenia was observed to be significantly diminished in the trastuzumab-**1** treatment relative to trastuzumab-**2** treatment. These pharmacological advantages suggest that the use of SSF in

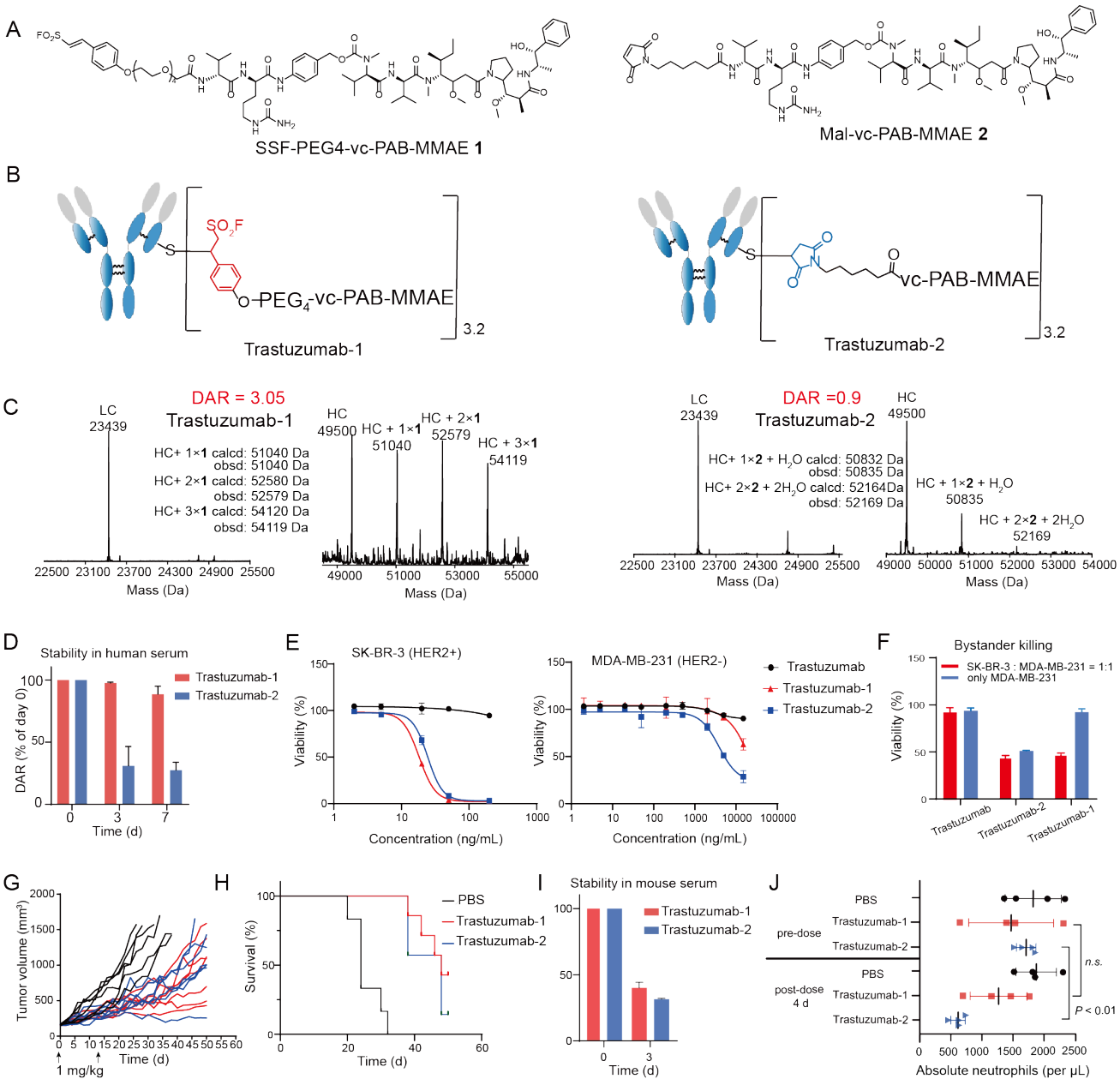

Figure 5. Construction of serum-stable ADC via SSF enabled Cys-specific modifications. A) Chemical structures of SSF and Mal-linked toxin (vc-PAB-MMAE). B) Structural comparison of trastuzumab-**1** and trastuzumab-**2**; D) stability studies of trastuzumab-**1** and trastuzumab-**2** in human serum. ADCs were incubated in human serum for 0, 3, and 7 days at 37°C. Shown MS specra (C) are the relative DAR changes after 7 days. LC: light chain, HC: heavy chain. E) Cell viability assays with HER2+ cell lines (SK-BR-3) and HER2- cell lines (MDA-MB-231) for assessing trastuzumab-**1**, trastuzumab-**2** and trastuzumab. F) Bystander killing effect of trastuzumab-**1** and trastuzumab-**2**. ADCs were performed in cell culture medium at 2 μg/mL final concentration for cocultured group and 5 μg/mL final concentration for only MDA-MB-231 group. G) Antitumor activity of trastuzumab-**1** and trastuzumab-**2** in an NCI-N87 tumor xenograft model in BALB/c nude mice. Tumor volumes of the seven mice per group are shown separately. H) Kaplan–Meier survival analysis of the study shown in (G). I) Stability studies of trastuzumab-**1** and trastuzumab-**2** in mouse serum. ADCs were incubated in mouse serum for 0, 3 days at 37°C. J) Neutropenia observed in rats following a 20 mg/kg ADC dose. Four animals were dosed with trastuzumab-**1**, trastuzumab-**2** or vehicle and sampled for hematology markers.

ADC construction may improve the efficacy and safety due to its high serum stability.

Construction of serum-stable DNA-protein conjugates via SSF-Cys conjugation

Recently, DNA-protein conjugates are widely used in diversified biomedical applications, *e.g.*, cellular indexing of transcriptomes and epitopes (CITE-seq) at single cell level[28] and DNA-PAINT based super-resolution imaging[29].

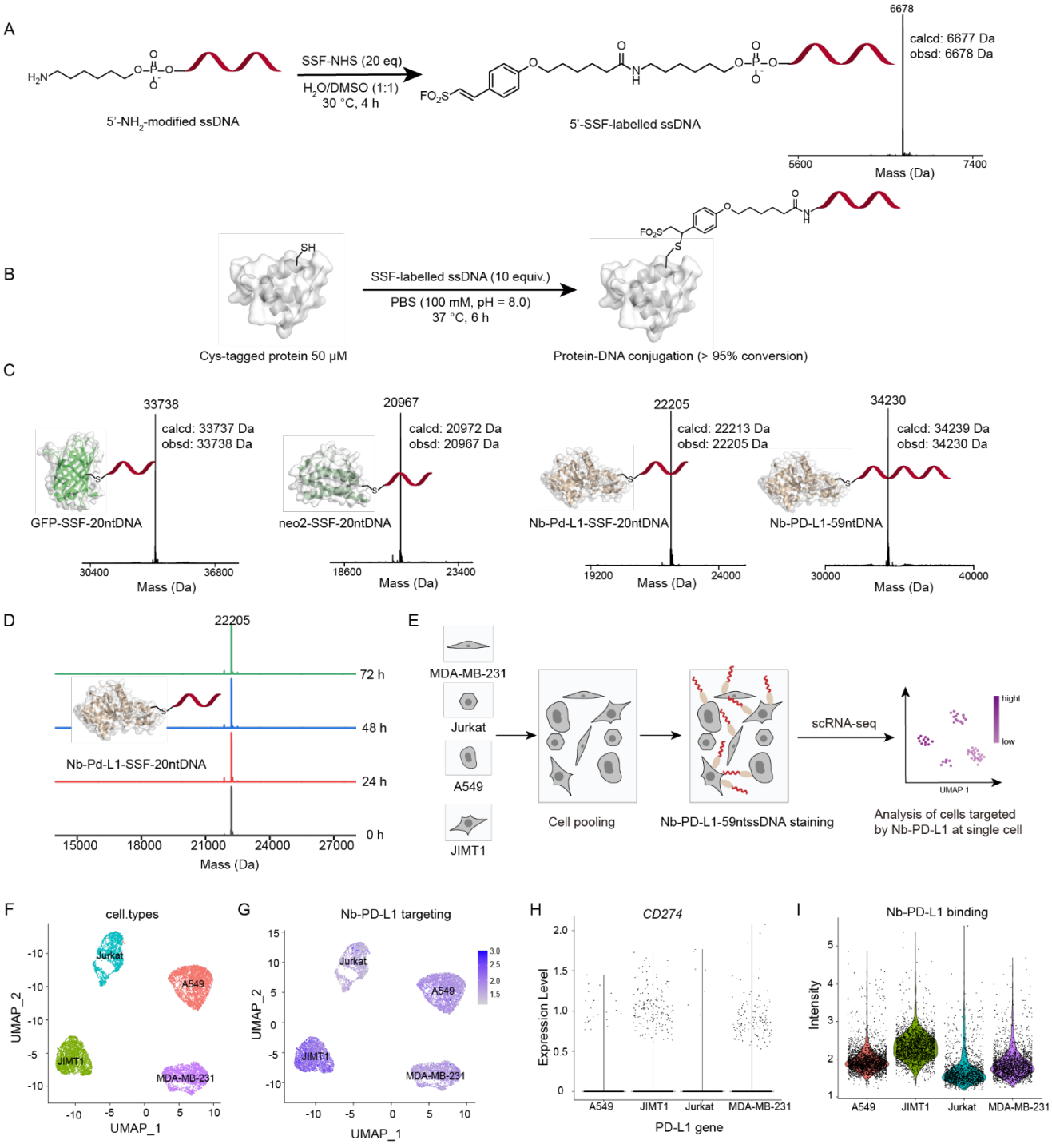

Figure 6. Construction of site-specific DNA-protein conjugates by SSF-ssDNA and the application of Nb-PD-L1 ssDNA in single-cell RNA sequencing. A) Modification of 5'-amino ssDNA with SSF-NHS. B) Scheme of protein modification with SSF-ssDNA probes. C) Deconvoluted mass spectra for DNA-protein conjugates constructed via 20nt SSF-ssDNA or 59nt SSF-ssDNA probes. D) LC-MS based conjugate integrity study of Nb-PD-L1-20ntssDNA in the presence of 10% human serum with deconvoluted mass spectra of samples taken at specified time points. (E) Schematic overview of Nb-PD-L1-ssDNA enabled CITE-seq for detecting targeted cells at single cell level with transcriptome. (F) Transcriptome-based clustering of single-cell expression profiles. Cyan: Jurkat; red: A549; green: JIMT-1; violet: MDA-MB-231. (G) Relative intensity of Nb-PD-L1-ssDNA targeting superimposed on the UMAP projections shown in (F). (H) Violin plot describing mRNA expression level of PD-L1 (*CD274*) in the four cell lines. (I) Violin plot describing scaled (z-score) normalized UMI counts of the 59nt-ssDNA barcode (Nb-PD-L1 binding intensity) in the four cell lines..

Readily available Cys-reactive oligonucleotides (oligos) are preferred in preparing DNA-protein conjugates. However, maleimide modified ssDNA has shown to be instable for long-time storage. To demonstrate the advantage of SSF in making stable Cys-reactive ssDNA probe， we synthesized SSF-NHS ester (structure in **SI**) and used this bifunctional cross-linker to successfully modify the 5' NH2 labeled ssDNA probe (**Fig. 6A**). Compared to maleimide-ssDNA, SSF-ssDNA was quite stable in alkaline buffer at 37 ℃ (**Fig. S13**). With the stable and readily reactive 5' SSF modified ssDNA on hand, we tried to label proteins of GFP, neo-2 and Nb-PD-L1 with a 20nt ssDNA probe. Successful modification of DNA-protein conjugates was characterized as a single product by LC-MS on all of these proteins (**Fig. 6B-C**). As a nanobody-DNA conjugate, Nb-PD-L1-ssDNA has much smaller size than antibody-DNA conjugate and could be potentially used for the purpose of targeted delivery of oligo drugs or signal-amplifiable antigen detection in deep tissue. Thus, we incubated this conjugate in PBS buffer contains 10 % human serum at 37 ℃ to determine its potential serum stability. LC-MS and SDS-PAGE analysis at different time points demonstrates that Nb-PD-L1-ssDNA is stable in the presence of human serum, even after 72h treatment (**Fig. 6D, Fig. S14**). CITE-seq is a single-cell sequencing based multiomic technique that allows the simultaneous detection of cell surface epitopes and transcriptomes at the single-cell level[5c-e]. In this platform, the ssDNA barcoded antibody that binds to the corresponding epitopes on cell surface could be detected in the commercial single-cell RNA sequencing (scRNA-seq). To demonstrate SSF enabled nanobody-DNA conjugate could be used in CITE-seq, we labeled Nb-PD-L1-ssDNA with a 59nt ssDNA barcode for detecting PD-L1 (**Fig. 6C, 6E**). A cell mixture of Jurkat, A549, JIMT-1 and MDA-MB-231 was stained with Nb-PD-L1-ssDNA and then subjected to the scRNA platform. Following common data processing procedure, we obtained a total of 8301 cells in final scRNA-seq dataset. We identified clusters in gene expression space according to known markers for Jurkat, A549, JIMT-1 as well as MDA-MB-231 cells (**Fig. 6F**, gene markers in **Fig. S15**). Projection of the Nb-PD-L1 barcode onto gene expression space was performed according to the unique molecular identifier (UMI) of the same cell (**Fig. 6G**). The PD-L1 antigen that could be targeted by this clonotype of nanobody was further quantified over four types of cells and summarized as shown in the violin plot, showing that JIMT-1 was the most targeted cell type by Nb-PD-L1 while Jurkat was the least targeted (**Fig. 6I**). By contrast, the mRNA encoding PD-L1 (*CD274*) showed neglectable signal and there was no significant difference between these cells (**Fig. 6H**), which might account to the low transcription under no stimulation. These results prove that SSF enabled Nb-PD-L1-ssDNA conjugate could help to identify targeted cell in scRNA-seq, which might be ignored when analysis is performed only according to the gene transcription.

CONCLUSION

In summary, we present SSF as a novel cysteine-specific bioconjugation reagent for the construction of diversified protein conjugates. Compared to maleimide, SSF displayed a balanced performance, or so-called "sweet spot", in the context of reactivity, selectivity and stability. In addition, the SO_2F group on the conjugate is stable in serum or GSH treatment. Although maleimide derived MAs or other type of electron-poor labeling reagents have been developed for stable protein conjugates construction[17c, 17h, 30], novel MAs with unique molecular structure, good self-stability and simple procedure of synthesis are still required. We believe that the discovery of SSF not only provides an important alternative approach to label protein specifically, but also expand the fragmental library for developing Cys-specific covalent inhibitors[31]. Noteworthily, the unexpected reactivity inconsistency on peptides and proteins inspires us to characterize reactions directly on proteins in the future, which may open the door of rediscovering protein chemistries from those misplaced reagents.

Since SSF is a near perfect MA for Cys-specific protein bioconjugation, we also show the great performance of SSF in functional protein conjugates construction as well as biomedical applications. ADCs with high DAR ratios (3.2 or 7.2) were successfully constructed from native antibodies with minimal SSF-toxin excesses in one-pot (**Fig 5, Fig S16**). Subsequent comprehensive comparisons show the great stability of the SSF derived ADC in human serum as well as its improved efficacy and safety in animal model. Meanwhile, SSF also allows the construction of DNA-protein conjugates via the readily reactive SSF-DNA probe in one-step, even when using a 59nt SSF-functionalized oligo barcode. Since the Nb-PD-L1 used here has been developed as the first subcutaneously administrated checkpoint inhibitor Envafolimab (KN035) in clinic[32], this Nb-PD-L1-ssDNA conjugate could potentially find broad applications for the *ex vivo* detection of targeted cells at the single-cell level in clinical tissue samples.SSF-Cys is stable in GSH treatment, we believe that trastuzumab-**1** could show higher stability than trastuzumab-**2**. To prove that under clinically relevant conditions, we next evaluated their stability in human plasma *in vitro* (**Fig. 7D-E, Fig. S10-11**). ADCs were incubated with human serum at 37°C for 7 days. After incubation, 90% of trastuzumab-**1** was still stable, while more than 70% of trastuzumab-**2** lost their payload. These plasma stability data confirm the exquisite stability of trastuzumab-**1**.

ASSOCIATED CONTENT

This material is available free of charge via the Internet at http://pubs.acs.org.
Complete experimental details and procedures, supporting figures, supporting tables, NMR spectra and MS spectra (PDF)

AUTHOR INFORMATION

Corresponding Author

Jieli@nju.edu.cn

Notes

The authors declare the following competing financial interest(s): The technology described in the manuscript is part of a pending patent application by Wu, Q.; Yang, Y.; Sha, W.; Li, J. Conjugate and the preparing method

and use. International application No. PCT/CN2021/086094, filed on Apr/9/2021.

ACKNOWLEDGMENT

Financial supports from the National Key R&D Program of China (2019YFA09006600), National Natural Science Foundation of China (21977048 and 92053111), Natural Science Foundation of Jiangsu Province (BK20202004), Beijing National Laboratory for Molecular Sciences (BNLMS202008), Jiangsu Specially-Appointed Professor Plan, Program for Innovative Talents and Entrepreneur in Jiangsu and are gratefully acknowledged. Q.Z. is the Connie and Bob Lurie Fellow of the Damon Runyon Cancer Research Foundation (DRG-2434-21). We thank Prof. Huali Qin for providing **MA10**, **MA11** and Alphamab Co. Ltd. for prividing KN026, KN046 as gifts.

REFERENCES

[1] G. C. Rudolf, W. Heydenreuter, S. A. Sieber, *Curr Opin Chem Biol* **2013**, *17*, 110-117.

[2] a) M. V. Tsurkan, K. Chwalek, S. Prokoph, A. Zieris, K. R. Levental, U. Freudenberg, C. Werner, *Adv. Mater.* **2013**, *25*, 2606-2610; b) E. A. Phelps, N. O. Enemchukwu, V. F. Fiore, J. C. Sy, N. Murthy, T. A. Sulchek, T. H. Barker, A. J. Garcia, *Adv. Mater.* **2012**, *24*, 64-70, 62; c) A. D. Baldwin, K. L. Kiick, *Polym. Chem.* **2013**, *4*, 133-143.

[3] L. Xue, I. A. Karpenko, J. Hiblot, K. Johnsson, *Nat. Chem. Biol.* **2015**, *11*, 917-923.

[4] S. Mohapatra, C. T. Lin, X. A. Feng, A. Basu, T. Ha, *Chem Rev* **2020**, *120*, 36-78.

[5] a) Y. Hao, S. Hao, E. Andersen-Nissen, W. M. Mauck, 3rd, S. Zheng, A. Butler, M. J. Lee, A. J. Wilk, C. Darby, M. Zager, P. Hoffman, M. Stoeckius, E. Papalexi, E. P. Mimitou, J. Jain, A. Srivastava, T. Stuart, L. M. Fleming, B. Yeung, A. J. Rogers, J. M. McElrath, C. A. Blish, R. Gottardo, P. Smibert, R. Satija, *Cell* **2021**, *184*, 3573-3587 e3529; b) M. Slyper, C. B. M. Porter, O. Ashenberg, J. Waldman, E. Drokhlyansky, I. Wakiro, C. Smillie, G. Smith-Rosario, J. Wu, D. Dionne, S. Vigneau, J. Jane-Valbuena, T. L. Tickle, S. Napolitano, M. J. Su, A. G. Patel, A. Karlstrom, S. Gritsch, M. Nomura, A. Waghray, S. H. Gohil, A. M. Tsankov, L. Jerby-Arnon, O. Cohen, J. Klughammer, Y. Rosen, J. Gould, L. Nguyen, M. Hofree, P. J. Tramontozzi, B. Li, C. J. Wu, B. Izar, R. Haq, F. S. Hodi, C. H. Yoon, A. N. Hata, S. J. Baker, M. L. Suva, R. Bueno, E. H. Stover, M. R. Clay, M. A. Dyer, N. B. Collins, U. A. Matulonis, N. Wagle, B. E. Johnson, A. Rotem, O. Rozenblatt-Rosen, A. Regev, *Nat Med* **2020**, *26*, 792-802; c) C. Zhu, S. Preissl, B. Ren, *Nat Methods* **2020**, *17*, 11-14; d) E. P. Mimitou, A. Cheng, A. Montalbano, S. Hao, M. Stoeckius, M. Legut, T. Roush, A. Herrera, E. Papalexi, Z. Ouyang, R. Satija, N. E. Sanjana, S. B. Koralov, P. Smibert, *Nat Methods* **2019**, *16*, 409-412; e) T. Stuart, R. Satija, *Nat Rev Genet* **2019**, *20*, 257-272; f) E. Papalexi, R. Satija, *Nat Rev Immunol* **2018**, *18*, 35-45; g) J. Lee, D. Y. Hyeon, D. Hwang, *Exp Mol Med* **2020**, *52*, 1428-1442. [6] R. J. Deshaies, *Nature* **2020**, *580*, 329-338.

[7] a) S. Y. Lin, X. Jia, Shang. Weeks, A, M. Hornsby, M. Lee, P, S. Nichiporuk, R, V. Iavarone, A, T. Wells, J, A. Toste, F. D. Chang, C, J., *Science* **2017**, *355*, 597-602; b) E. A. Hoyt, P. M. S. D. Cal, B. L. Oliveira, G. J. L. Bernardes, *Nat. Rev. Chem.* **2019**, *3*, 147-171; c) N. Stephanopoulos, M. B. Francis, *Nat. Chem. Biol.* **2011**, *7*, 876-884; d) N. Krall, F. P. da Cruz, O. Boutureira, G. J. Bernardes, *Nat. Chem.* **2016**, *8*, 103-113; e) V. Chudasama, A. Maruani, S. Caddick, *Nat. Chem.* **2016**, *8*, 114-119; f) M. J. Matos, B. L. Oliveira, N. Martinez-Saez, A. Guerreiro, P. Cal, J. Bertoldo, M. Maneiro, E. Perkins, J. Howard, M. J. Deery, J. M. Chalker, F. Corzana, G. Jimenez-Oses, G. J. L. Bernardes, *J. Am. Chem. Soc.* **2018**, *140*, 4004-4017.

[8] P. Ochtrop, C. P. R. Hackenberger, *Curr. Opin. Chem. Biol.* **2020**, *58*, 28-36.

[9] a) J. M. Chalker, G. J. Bernardes, Y. A. Lin, B. G. Davis, *Chem. Asian. J.* **2009**, *4*, 630-640; b) S. B. Gunnoo, A. Madder, *Chembiochem* **2016**, *17*, 529-553.

[10] S. Sechi, B. T. Chait, *Anal. Chem.* **1998**, *70*, 5150-5158.

[11] C. Zhang, E. V. Vinogradova, A. M. Spokoyny, S. L. Buchwald, B. L. Pentelute, *Angew. Chem. Int. Ed.* **2019**, *58*, 4810-4839.

[12] J. Ravasco, H. Faustino, A. Trindade, P. M. P. Gois, *Chem. Eur.* **2019**, *25*, 43-59.

[13] I. Nessler, B. Menezes, G. M. Thurber, *Trends. Pharmacol. Sci.* **2021**, *42*, 803-812.

[14] J. D. Gregory, *J. Am. Chem. Soc.* **1955**, *77*, 3922-3923.

[15] A. Mukhortava, M. Schlierf, *Bioconjug Chem* **2016**, *27*, 1559-1563.

[16] B. Q. Shen, K. Xu, L. Liu, H. Raab, S. Bhakta, M. Kenrick, K. L. Parsons-Reponte, J. Tien, S. F. Yu, E. Mai, D. Li, J. Tibbitts, J. Baudys, O. M. Saad, S. J. Scales, P. J. McDonald, P. E. Hass, C. Eigenbrot, T. Nguyen, W. A. Solis, R. N. Fuji, K. M. Flagella, D. Patel, S. D. Spencer, L. A. Khawli, A. Ebens, W. L. Wong, R. Vandlen, S. Kaur, M. X. Sliwkowski, R. H. Scheller, P. Polakis, J. R. Junutula, *Nat. Biotechnol.* **2012**, *30*, 184-189.

[17] a) R. Huang, Z. Li, Y. Sheng, J. Yu, Y. Wu, Y. Zhan, H. Chen, B. Jiang, *Org. Lett.* **2018**, *20*, 6526-6529; b) E. V. Vinogradova, C. Zhang, A. M. Spokoyny, B. L. Pentelute, S. L. Buchwald, *Nature* **2015**, *526*, 687-691; c) R. P. Lyon, J. R. Setter, T. D. Bovee, S. O. Doronina, J. H. Hunter, M. E. Anderson, C. L. Balasubramanian, S. M. Duniho, C. I. Leiske, F. Li, P. D. Senter, *Nat. Biotechnol.* **2014**, *32*, 1059-1062; d) H. Seki, S. J. Walsh, J. D. Bargh, J. S. Parker, J. Carroll, D. R. Spring, *Chem. Sci.* **2021**, *12*, 9060-9068; e) N. Toda, S. Asano, C. F. Barbas, 3rd, *Angew. Chem. Int. Ed.* **2013**, *52*, 12592-12596; f) C. E. Stieger, L. Franz, F. Korlin, C. P. R. Hackenberger, *Angew. Chem. Int. Ed.* **2021**, *60*, 15359-15364; g) V. Laserna, D. Abegg, C. F. Afonso, E. M. Martin, A. Adibekian, P. Ravn, F. Corzana, G. J. L. Bernardes, *Angew. Chem. Int. Ed.* **2021**, *60*, 23750-23755; h) M. A. Kasper, A. Stengl, P. Ochtrop, M. Gerlach, T. Stoschek, D. Schumacher, J. Helma, M. Penkert, E. Krause, H. Leonhardt, C. P. R. Hackenberger, *Angew. Chem. Int. Ed.* **2019**, *58*, 11631-11636.

[18] A. M. ElSohly, M. B. Francis, *Acc Chem Res* **2015**, *48*, 1971-1978.

[19] D. S. Allgauer, H. Jangra, H. Asahara, Z. Li, Q. Chen, H. Zipse, A. R. Ofial, H. Mayr, *J. Am. Chem. Soc.* **2017**, *139*, 13318-13329.

[20] For a comprehensive database of nucleophilicity parameters N, sN, and electrophilicity parameters E, see http://www.cup.lmu.de/oc/mayr/DBintro.html.

[21] a) J. Dong, L. Krasnova, M. G. Finn, K. B. Sharpless, *Angew. Chem. Int. Ed.* **2014**, *53*, 9430-9448; b) G. F. Zha, Q. Zheng, J. Leng, P. Wu, H. L. Qin, K. B. Sharpless, *Angew. Chem. Int. Ed.* **2017**, *56*, 4849-4852; c) J. Leng, N. S. Alharbi, H.-L. Qin, *Eur. J. Org. Chem.* **2019**, *2019*, 6101-6105; d) Y.-M. Huang, S.-M. Wang, J. Leng, B. Moku, C. Zhao, N. S. Alharbi, H.-L. Qin, *Eur. J. Org. Chem.* **2019**, *2019*, 4597-4603; e) Q. Zheng, J. Dong, K. B. Sharpless, *J. Org. Chem.* **2016**, *81*, 11360-11362.

[22] a) Q. Chen, P. Mayer, H. Mayr, *Angew. Chem. Int. Ed.* **2016**, *55*, 12664-12667; b) R. J. Mayer, A. R. Ofial, *Angew. Chem. Int. Ed.* **2019**, *58*, 17704-17708.

[23] D. A. Silva, S. Yu, U. Y. Ulge, J. B. Spangler, K. M. Jude, C. Labao-Almeida, L. R. Ali, A. Quijano-Rubio, M. Ruterbusch, I. Leung, T. Biary, S. J. Crowley, E. Marcos, C. D. Walkey, B. D. Weitzner, F. Pardo-Avila, J. Castellanos, L. Carter, L. Stewart, S. R. Riddell, M. Pepper, G. J. L. Bernardes, M. Dougan, K. C. Garcia, D. Baker, *Nature* **2019**, *565*, 186-191.

[24] H. Zhang, Y. Han, Y. Yang, F. Lin, K. Li, L. Kong, H. Liu, Y. Dang, J. Lin, P. R. Chen, *J Am Chem Soc* **2021**, *143*, 16377-16382.

[25] C. A. Hudis, *N Engl J Med* **2007**, *357*, 39-51.

[26] J. Zhang, D. Ji, L. Cai, H. Yao, M. Yan, X. Wang, W. Shen, Y. Du, H. Pang, X. Lai, H. Zeng, J. Huang, Y. Sun, X. Peng, J. Xu, J. Yang, F. Yang, T. Xu, X. Hu, *Clin Cancer Res* **2022**, *28*, 618-628.

[27] t. D. Xu, Y. Wang, P. Chen. T, *Patent US 2018/0291103* **2016**.

[28] M. Stoeckius, C. Hafemeister, W. Stephenson, B. Houck-Loomis, P. K. Chattopadhyay, H. Swerdlow, R. Satija, P. Smibert, *Nat Methods* **2017**, *14*, 865-868.

[29] a) R. Jungmann, M. S. Avendano, J. B. Woehrstein, M. Dai, W. M. Shih, P. Yin, *Nat Methods* **2014**, *11*, 313-318; b) S. S. Agasti, Y. Wang, F. Schueder, A. Sukumar, R. Jungmann, P. Yin, *Chem Sci* **2017**, *8*, 3080-3091; c) T. Schlichthaerle, A. S. Eklund, F. Schueder, M. T. Strauss, C. Tiede, A. Curd, J. Ries, M. Peckham, D. C. Tomlinson, R. Jungmann, *Angew Chem Int Ed Engl* **2018**, *57*, 11060-11063; d) J. Konc, L. Brown, D. R. Whiten, Y. Zuo, P. Ravn, D. Klenerman, G. J. L. Bernardes, *Angew Chem Int Ed Engl* **2021**, *60*, 25905-25913.

[30] a) W. Huang, X. Wu, X. Gao, Y. Yu, H. Lei, Z. Zhu, Y. Shi, Y. Chen, M. Qin, W. Wang, Y. Cao, *Nat Chem* **2019**, *11*, 310-319; b) D. Kalia, P. V. Malekar, M. Parthasarathy, *Angew Chem Int Ed Engl* **2016**, *55*, 1432-1435; c) B. Bernardim, P. M. Cal, M. J. Matos, B. L. Oliveira, N. Martinez-Saez, I. S. Albuquerque, E. Perkins, F. Corzana, A. C. Burtoloso, G. Jimenez-Oses, G. J. Bernardes, *Nat. Commun.* **2016**, *7*, 13128-131337; d) P. A. Szijj, C. Bahou, V. Chudasama, *Drug Discov Today Technol* **2018**, *30*, 27-34.

[31] a) B. R. Lanning, L. R. Whitby, M. M. Dix, J. Douhan, A. M. Gilbert, E. C. Hett, T. O. Johnson, C. Joslyn, J. C. Kath, S. Niessen, L. R. Roberts, M. E. Schnute, C. Wang, J. J. Hulce, B. Wei, L. O. Whiteley, M. M. Hayward, B. F. Cravatt, *Nat Chem Biol* **2014**, *10*, 760-767; b) K. Senkane, E. V. Vinogradova, R. M. Suciu, V. M. Crowley, B. W. Zaro, J. M. Bradshaw, K. A. Brameld, B. F. Cravatt, *Angew Chem Int Ed* **2019**, *58*, 11385-11389.

[32] F. Zhang, H. Wei, X. Wang, Y. Bai, P. Wang, J. Wu, X. Jiang, Y. Wang, H. Cai, T. Xu, A. Zhou, *Cell Discov* **2017**, *3*, 17004

Identification of Styryl Sulfonyl Fluoride (SSF) as An Efficient, Robust and Irreversible Cysteine-specific Protein Bioconjugation Reagent